Inorg. Chem. **2006**, *45*, 8442–8446

Molecular Structures of *Arachno*-Heteroboranes with Decaborane Frameworks: Two C_s-symmetrical Azacarba- and Carbathiaboranes

Drahomír Hnyk,[†] Josef Holub,[†] Stuart A. Hayes,[‡] Mark F. Robinson,[‡] Derek A. Wann,[‡] Heather E. Robertson,[‡] and David W. H. Rankin*[,‡]

Institute of Inorganic Chemistry, Academy of Sciences of the Czech Republic, 25068 Řež, Czech Republic and School of Chemistry, University of Edinburgh, West Mains Road, Edinburgh, EH9 3JJ, U.K.

Received July 6, 2006

The gas-phase structure of 6,9-CSB_8H_{12} has been determined by electron diffraction and ab initio calculations, and that of 6,9-CNB_8H_{13} has also been calculated. The accuracy of each structure has been confirmed by ^{11}B NMR calculations. The position of the sulfur atom is very close to that of the boron atom occupying the equivalent position in the parent molecule $[B_{10}H_{14}]^{2-}$, reflecting the similarity of sizes of sulfur and boron atoms. The nitrogen and carbon atoms, on the other hand, lie much closer to the centers of the cages. The B(8)–X(9)–B(10) angles increase from 98.7° for X = S to 122.8° for X = N. There are also large changes in relative lengths of bonds, with some bonds lengthening by up to 14.6 pm on introduction of a sulfur atom.

Introduction

Systematic replacement of $\{BH_2\}$- vertexes in [*arachno*-$B_{10}H_{14}]^{2-}$ (Figure 1, **1**)[1] by isoelectrolobal[2] units such as $\{CH_2\}$, {NH}, and {S} can lead to a variety of ten-vertex *arachno* heteroboranes. These range from monoheteroatomic species, exemplified by $[6\text{-}CB_9H_{14}]^-$,[3] $[6\text{-}NB_9H_{13}]^-$,[4] and $[6\text{-}SB_9H_{12}]^-$,[5] to compounds in which the decaborane framework incorporates more than one electron-rich center. Such diheteroatomic two-vertex substitution complexes can be divided into two classes: those in which a single heteroatom appears twice (e.g., 6,9-$C_2B_8H_{14}$,[6] 6,9-$N_2B_8H_{12}$,[7] and 6,9-$Se_2B_8H_{10}$;[8] 6,9-$S_2B_8H_{10}$, however, has never been synthesized) or with mixed heteroatoms (e.g. 6,9-CNB_8H_{13}, **2**,[9] and 6,9-CSB_8H_{12}, **3**,[9] shown in Figures 2 and 3, respectively). Both mono- and diheteroatomic structures are in accordance with Gimarc's topological rule,[10] which states that elements more electronegative than boron (C, N, S) prefer to occupy the cluster sites with the highest electron

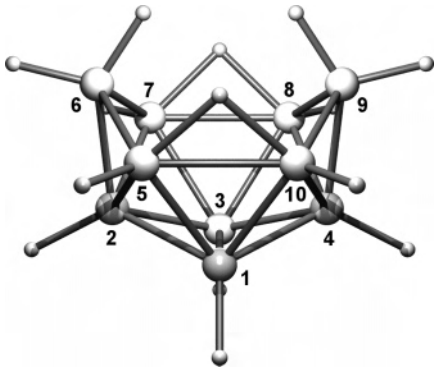

Figure 1. Molecular structure of [*arachno*-$B_{10}H_{14}]^{2-}$, **1**, showing boron numbering.

* To whom correspondence should be addressed. E-mail: d.w.h.rankin@ed.ac.uk.
[†] Academy of Sciences of the Czech Republic.
[‡] University of Edinburgh.

(1) Kendall, D. S.; Lipscomb W. N. *Inorg. Chem.* **1973**, *12*, 546 and references therein.
(2) For a definition of isoelectrolobal, see, for example: Beckett, M. A.; Crook, J. E.; Greenwood, N. N.; Kennedy, J. D. *J. Chem. Soc., Dalton Trans.* **1986**, 1879.
(3) Fontaine, X. L. R.; Kennedy, J. D.; Thornton-Pett, M.; Nestor, K.; Štíbr, B.; Jelínek, T.; Baše, K. *J. Chem. Soc., Dalton Trans.* **1990**, 2887.
(4) (a) Hertler, W. R.; Klanberg, F.; Muetterties, E. L. *Inorg. Chem.* **1967**, *6*, 1696. (b) Baše, K.; Hanousek, F.; Štíbr, B.; Plešek, J.; Lyčka, J. *J. Chem. Soc., Chem. Commun.* **1981**, 1163. (c) Baše, K. *Collect. Czech. Chem. Commun.* **1983**, *48*, 2593.
(5) (a) Rudolph, R. W.; Pretzer, R. W. *Inorg. Synth.* **1983**, *22*, 226. (b) Siedle, A. R.; Bodner, G. M.; Garber, A. R.; McDowell, D.; Todd, L. J. *Inorg. Chem.* **1977**, *13*, 1756. (c) Bown, M.; Fontaine, X. L. R.; Kennedy, J. D. *J. Chem. Soc., Dalton Trans.* **1988**, 1467.
(6) Štíbr, B.; Plešek, J.; Heřmánek, S. *Collect. Czech. Chem. Commun.* **1974**, *39*, 1805.
(7) Štíbr, B.; Kennedy, J. D.; Jelínek, T. *J. Chem. Soc., Chem. Commun.* **1990**, 1309.
(8) Friesen, G. D.; Barriola, A.; Todd, L. J. *Chem. Ind.* **1978**, 631.
(9) Holub, J.; Jelínek, T.; Plešek, J.; Štíbr, B.; Heřmánek, S.; Kennedy, J. *J. Chem. Soc., Chem. Commun.* **1991**, 1389.
(10) Ott, J. J.; Gimarc, B. M. *J. Am. Chem. Soc.* **1986**, *108*, 4303.

10.1021/ic061253h CCC: $33.50
Published on Web 09/09/2006

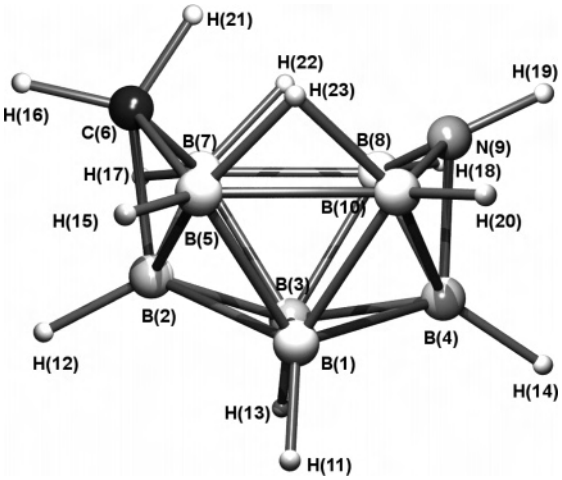

Figure 2. Molecular structure of *arachno*-6,9-CNB_8H_{13}, **2**.

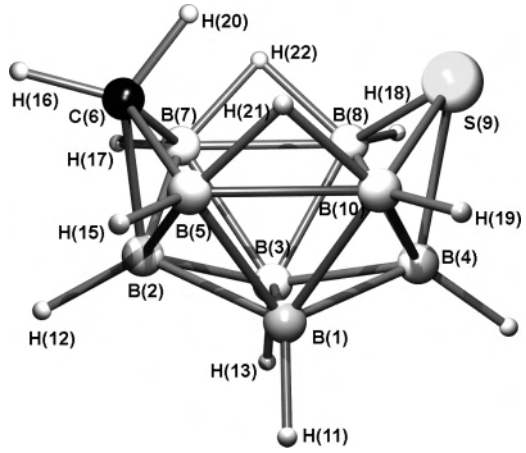

Figure 3. Molecular structure of *arachno*-6,9-CSB_8H_{13}, **3**.

density. Natural population analysis (NPA) has shown that for **1** these sites correspond to boron atoms 6 and 9. (See Figure 1 for atom numbering.)[11] The structures of the C_{2v}-symmetric dicarba-, diaza-, and diselenaboranes have been determined by the ab initio/GIAO/NMR method[12] and, in the case of 6,9-$C_2B_8H_{14}$, by gas-phase electron diffraction.[13] However, no structural studies have been performed for the mixed diheteroatomic 10-vertex *arachno* systems in any phase. To broaden our knowledge of the structural effects upon substituting the parent **1**, we have undertaken computational studies of **2** and **3**. The latter has also been studied by gas-phase electron diffraction.

Experimental Section

Computational Details. All calculations were performed using the Gaussian 03 program package[14] on a Fujitsu Siemens PC. Structures for **2** and **3** were first optimized at the RHF/6-31G* level of theory with symmetry constraints (C_s). Second-derivative analysis, carried out at the same level, determined the nature of the stationary points: both structures displayed one minimum without imaginary frequencies. Optimization at the RMP2(fc)/6-31G* level included the effects of electron correlation. The size of the basis set was then increased sequentially to 6-311++G**. Both the RMP2/6-311++G** geometry and the RMP2/6-31G* geometry were used for calculations of chemical shieldings (the latter to facilitate comparisons with previous structural characterizations). These were calculated at SCF and MP2 levels with the GIAO method and employed II′ (TZP, DZ, on H) and II (TZP) Huzinaga basis sets,[15] well-designed for calculation of magnetic properties. Coordinates for the RMP2(fc)/6-31G* structures of **2** and **3** and the RMP2(fc)/6-311++G** structure for **3** are available as Supporting Information (Tables S1−S3). Wiberg bond indices[16] were calculated for **1**, **2**, and **3** using the NBO program[17] incorporated into Gaussian03.

Gas Electron Diffraction. A sample of **3** was prepared according to the literature procedure.[9] Data were collected on Kodak Electron Image film using the Edinburgh gas electron diffraction apparatus,[18] with an accelerating voltage of ca. 40 kV (ca. 6.0 pm electron wavelength). Nozzle-to-film distances were calculated using benzene vapor as a standard, immediately after recording the diffraction

(11) (a) For well-known drawbacks of the Mulliken approach, see, for example: Reed, A. E.; Weinstock, R. B.; Weinhold, F. *J. Chem. Phys.* **1985**, *83*, 735. Using Mulliken charges resulted in a different charge distribution within **1** as compared with the NPA picture, B(6, 9) being the most negative (−0.309) according to the latter approach. (b) Also, in **1**, the B(8)−B(9) bond length and the B(8)−B(9)−B(10) angle were computed to be 189.4 pm and 101.5°, respectively. The B(5)−B(10) and B(4)−B(9) separations converged to 186.7 and 174.9 pm [RMP2-(fc)/6-31G*]. For all these results, see: Hnyk, D.; Holub, J. *Collect. Czech. Chem. Commun.* **2002**, *67*, 813.

(12) (a) Bühl, M.; Schleyer, P. v. R. *J. Am. Chem. Soc.* **1992**, *114*, 477. Examples of the ab initio/IGLO/NMR approach include: (b) A C_1 form of B_5H_{11} is favored over the C_s structure: Schleyer, P. v. R.; Bühl, M.; Fleischer, U.; Koch, W. *Inorg. Chem.* **1990**, *29*, 153. (c) The structure of *nido*-$C_2B_6H_{10}$: Bausch, J. W.; Prakash, G. K. S.; Bühl, M.; Schleyer, P. v. R.; Williams, R. E. *Inorg. Chem.* **1992**, *31*, 3060. (d) A theoretical and experimental refinement of *closo*-1-$NB_{11}H_{12}$: Hnyk, D.; Bühl, M.; Schleyer, P. v. R.; Volden, H. V.; Gundersen, S.; Müller, J.; Paetzold, P. *Inorg. Chem.* **1993**, *32*, 2442. For further references, see: (e) Bühl, M.; Schleyer, P. v. R. in: *Electron Deficient Boron and Carbon Clusters*; Olah, G. A., Wade, K., Williams, R. E., Eds.; Wiley: New York, 1991; Chapter 4, p 113. (f) Diaz, M.; Jaballas, T.; Arias, J.; Lee, H.; Onak, T. *J. Am. Chem. Soc.* **1996**, *118*, 4405 and references therein. (g) Bühl, M. *NMR* Chemical Shift Computation: Structural Applications. In *Encyclopedia of Computational Chemistry*; Schleyer, P. v. R., Allinger, N. L., Clark, T., Gasteiger, J., Kollman, P. A., Schaefer, H. F., Schreiner, P. R., Eds.; John Wiley and Sons: Chichester, UK, 1998; Vol. 3, p 1835. The most recent applications of the ab initio/GIAO/NMR method: (h) Holub, J.; Jelínek, T.; Hnyk, D.; Plzák, Z.; Císařová, I.; Bakardjiev, M.; Štíbr, B. *Chem. Eur. J.* **2001**, *7*, 1546. (i) Štíbr, B.; Tok, O. L.; Milius, W.; Bakardjiev, M.; Holub, J.; Hnyk, D.; Wrackmeyer, B. *Angew. Chem., Int. Ed.* **2002**, *41*, 2126.

(13) Hnyk, D.; Bühl, M.; Holub, J.; Hayes, S. A.; Wann, D. A.; Mackie, I. D.; Borisenko, K. B.; Robertson, H. E.; Rankin, D. W. H. *Inorg. Chem.* **2006**, *45*, 6014.

(14) Frisch, M. J.; Trucks, G. W.; Schlegel, H. B.; Scuseria, G. E.; Robb, M. A.; Cheeseman, J. R.; Montgomery, J. A., Jr.; Vreven, T.; Kudin, K. N.; Burant, J. C.; Millam, J. M.; Iyengar, S. S.; Tomasi, J.; Barone, V.; Mennucci, B.; Cossi, M.; Scalmani, G.; Rega, N.; Petersson, G. A.; Nakatsuji, H.; Hada, M.; Ehara, M.; Toyota, K.; Fukuda, R.; Hasegawa, J.; Ishida, M.; Nakajima, T.; Honda, Y.; Kitao, O.; Nakai, H.; Klene, M.; Li, X.; Knox, J. E.; Hratchian, H. P.; Cross, J. B.; Bakken, V.; Adamo, C.; Jaramillo, J.; Gomperts, R.; Stratmann, R. E.; Yazyev, O.; Austin, A. J.; Cammi, R.; Pomelli, C.; Ochterski, J. W.; Ayala, P. Y.; Morokuma, K.; Voth, G. A.; Salvador, P.; Dannenberg, J. J.; Zakrzewski, V. G.; Dapprich, S.; Daniels, A. D.; Strain, M. C.; Farkas, O.; Malick, D. K.; Rabuck, A. D.; Raghavachari, K.; Foresman, J. B.; Ortiz, J. V.; Cui, Q.; Baboul, A. G.; Clifford, S.; Cioslowski, J.; Stefanov, B. B.; Liu, G.; Liashenko, A.; Piskorz, P.; Komaromi, I.; Martin, R. L.; Fox, D. J.; Keith, T.; Al-Laham, M. A.; Peng, C. Y.; Nanayakkara, A.; Challacombe, M.; Gill, P. M. W.; Johnson, B.; Chen, W.; Wong, M. W.; Gonzalez, C.; Pople, J. A. *Gaussian 03*, revision B.03; Gaussian, Inc.: Wallingford, CT, 2004.

(15) Huzinaga, S. *Approximate Atomic Wave Functions*; University of Alberta: Edmonton, Canada, 1971.

(16) Wiberg, K. *Tetrahedron* **1968**, *24*, 1083.

(17) Glendening, E. D.; Reed, A. E.; Carpenter, J. E.; Weinhold, F. *NBO Version 3.1*.

(18) Huntley, C. M.; Laurenson, G. S.; Rankin, D. W. H. *J. Chem. Soc., Dalton Trans.* **1980**, 954.

Table 1. GED (r_{H1}) and Theoretical Molecular Parameters[a]

independent parameter	description	GED	MP2/6-311++G**[b]
p_1	rH average	122.3(2)	120.9
p_2	rB−H_b average minus B/C−H_t average	15.0(5)	15.3(5)
p_3	rB(5)−H(21) minus B(10)−H(21)	4.9(5)	4.9(5)
p_4	rB−H_t average minus C−H average	9.9(5)	9.7(5)
p_5	rC−H(20) minus C−H(16)	0.4(2)	0.4(2)
p_6	rB−B/C/S average	181.7(1)	181.3
p_7	rB−B average minus B−C average	9.7(2)	9.4(2)
p_8	rB−S average minus B−B average	13.6(3)	13.3(5)
p_9	rC−B(5) minus C−B(2)	8.3(4)	8.1(5)
p_{10}	rS−B(4) minus S−B(8)	0.2(5)	0.6(5)
p_{11}	rB−B difference 1[c]	8.0(1)	7.9(1)
p_{12}	rB−B difference 2[d]	2.1(2)	1.9(2)
p_{13}	rB−B difference 3[e]	6.3(3)	6.1(3)
p_{14}	rB(1)−B(4) minus B(1)−B(2)	1.3(2)	1.3(2)
p_{15}	rB(1)−B(10) minus B(2)−B(5)	0.9(2)	0.9(2)
p_{16}	rB(1)−B(5) minus B(1)−B(3)	1.6(2)	1.7(2)
p_{17}	rB(4)−B(10) minus B(5)−B(10)	5.3(5)	5.3(5)
p_{18}	∠O−B(2)−C[f]	116.4(3)	116.1
p_{19}	∠[180° minus B(2)−O−B(4)][f]	35.1(2)	35.4
p_{20}	∠H(12)−B(2)-C	112.2(5)	112.2(5)
p_{21}	∠H(14)−B(4)−S	116.1(5)	116.1(5)
p_{22}	∠H(16)−C−B(2)	111.9(5)	111.8(5)
p_{23}	∠H(20)−C−B(2)	135.9(5)	136.0(5)
p_{24}	∠H(11)−B(1)−B(3)	120.5(2)	120.5(2)
p_{25}	ϕH(11)−B(1)−B(3)−B(2)	109.0(5)	109.1(5)
p_{26}	∠H(15)−B(5)−B(1)	118.3(2)	118.2(2)
p_{27}	ϕH(15)−B(5)−B(1)−B(2)	107.3(8)	107.5(10)
p_{28}	∠H(19)−B(10)−B(1)	120.8(5)	120.8(5)
p_{29}	ϕH(19)−B(10)−B(1)−B(4)	−104.9(9)	−104.7(10)
p_{30}	∠B(7)···B(5)−H(21)	103.7(8)	103.5(10)

[a] Distances are in pm, and angles are in degrees. [b] Where theoretical values are followed by parentheses, the independent parameter was restrained to this value in the GED refinement with an uncertainty indicated in brackets. [c] {[B(1)−B(3)] + 2[B(1)−B(5)] + 2[B(5)−B(10)] + 2[B(4)−B(10)]}/7 − {[B(1)−B(2)] + [B(1)−B(4)] + [B(2)−B(5)] + [B(1)−B(10)]}/4. [d] {[B(1)−B(2)] + [B(1)−B(4)]}/2 − {[B(2)−B(5)] + [B(1)−B(10)]}/2. [e] {[B(1)−B(3)] + 2[B(1)−B(5)]}/3 − {[B(5)−B(10)] + [B(4)−B(10)]}/2. [f] O is the model origin, defined as the midpoint of B(1)−B(3).

pattern for **3**. Respective sample and nozzle temperatures of 409 and 441 K were used at the medium nozzle-to-film distance (204.2 mm), and those at the long nozzle-to-film distance (262.0 mm) were 394 and 415 K. The electron-scattering patterns were converted into digital form using an Epson Expression 1680 Pro flatbed scanner with a scanning program described previously.[19] Data reduction and least-squares refinements were carried out using the ed@ed program,[20] employing the scattering factors of Ross et al.[21] The scale factors, s limits, weighting points, correlation parameters, and electron wavelengths are provided as Supporting Information (Table S4).

A molecular model was written for **3**, converting a set of refineable, independent parameters into Cartesian atomic coordinates. This model was constructed assuming C_s symmetry (as exhibited by the calculated geometries and ^{11}B NMR experimental data), allowing the structure to be defined in terms of 30 independent parameters (p_1−p_{30}, Table 1). The heavy-atom cage was described using the average of all the B−B, B−C, and B−S distances (p_6) and 11 differences (p_7−p_{17}). The remaining two degrees of freedom were provided by the angle O···B(2)−C(6) (p_{18}), and a fold angle defined as 180° minus B(2)···O···B(4) (p_{19}). [In both cases, O denotes the origin, defined as the midpoint of B(1) and B(3).] The average of all bonded distances to hydrogen was used in the model (p_1). This, in combination with the difference between the average terminal hydrogen (H_t) and average bridging hydrogen (H_b) distances (p_2), allowed these two distances to be defined. The difference between the two B−H_b distances (p_3) then allowed both of these to refine. On the basis of the ab initio calculations, only one B−H_t distance was required. This was derived using the difference between B−H_t and the average C−H distance (p_4). The difference between C−H(16) and C−H(20) (p_5) allowed these two bond lengths to be found.

The positions of the hydrogen atoms lying in the plane of symmetry (numbers 12, 14, 16, and 20) were defined using angles made with the heavy-cage atoms (p_{20}, p_{21}, p_{22}, and p_{23}, respectively). Similarly, three angles (p_{24}, p_{26}, and p_{28}) and three torsional angles (p_{25}, p_{27}, and p_{29}) made with the cage were used to define the respective positions of the terminal hydrogen atoms, H(11), H(15), and H(19). Finally, the bridging hydrogen atoms were positioned using the angle B(7)···B(5)−H(21) (p_{30}).

GED Refinement. The GED refinement was performed using the SARACEN method[22] incorporating flexible restraints. A Cartesian force field was obtained from the RHF/6-31G* calculation and converted to a force field described by a set of symmetry coordinates using the program SHRINK.[23] From this, the root-mean-squared amplitudes of vibration (u_{h1}) and perpendicular distance corrections (k_{h1}) were generated.

(19) Fleischer, H.; Wann, D. A.; Hinchley, S. L.; Borisenko, K. B.; Lewis, J. R.; Mawhorter, R. J.; Robertson, H. E.; Rankin, D. W. H. *Dalton Trans.* **2005**, 3221.
(20) Hinchley, S. L.; Robertson, H. E.; Borisenko, K. B.; Turner, A. R.; Johnston, B. F.; Rankin, D. W. H.; Ahmadian, M.; Jones, J. N.; Cowley, A. H. *Dalton Trans.* **2004**, 2469.
(21) Ross, A. W.; Fink, M.; Hilderbrandt, R. *International Tables for Crystallography*; Wilson, A. J. C., Ed.; Kluwer Academic Publishers: Dordrecht, Boston, and London, 1992; Vol. C, p 245.
(22) (a) Mitzel, N. W.; Smart, B. A.; Blake, A. J.; Robertson, H. E.; Rankin D. W. H. *J. Phys. Chem.* **1996**, *100*, 9339. (b) Blake, A. J.; Brain, P. T.; McNab, H.; Miller, J.; Morrison, C. A.; Parsons, S.; Rankin, D. W. H.; Robertson, H. E.; Smart, B. A. *J. Phys. Chem.* **1996**, *100*, 12280. (c) Mitzel, N. W.; Rankin, D. W. H. *Dalton Trans.* **2003**, 3650.
(23) Sipachev, V. A. *J. Mol. Struct.* (*THEOCHEM*) **1985**, *121*, 143.

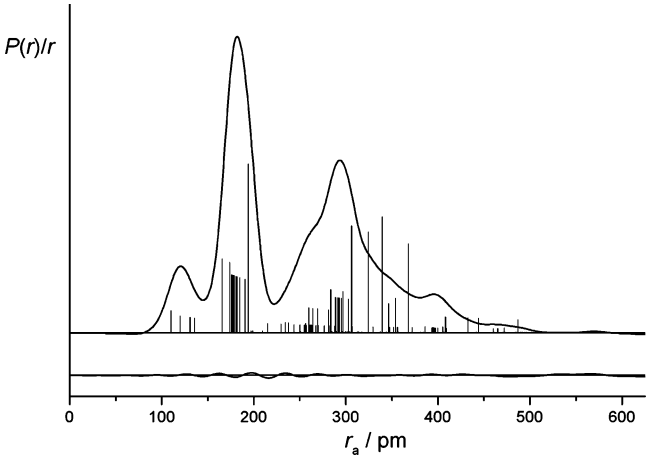

Figure 4. Experimental and difference (experimental minus theoretical) radial-distribution curves, $P(r)/r$, for **3**. Before Fourier inversion the data were multiplied by $s \exp[(-0.00002s^2)/(Z_S - f_S)(Z_C - f_C)]$.

All 30 independent parameters were refined, 26 of which were restrained to the values calculated at MP2/6-311++G**. Nine groups of amplitudes of vibrations were also refined, all of which were restrained to their RHF/6-31G* values. Eight of these groups of amplitudes were restrained with uncertainties of 10% of their values and the remaining group, corresponding to the heavy-atom bonded distances, with an uncertainty of 5%. A full list of interatomic distances, amplitudes of vibration and perpendicular distance corrections are given in Table S5.

The final refinement produced an R factor (R_G) of 0.037 (R_D = 0.019). A qualitative assessment of the fit can also be obtained by observing the radial-distribution and molecular-intensity scattering curves (Figures 4 and S1, respectively), which show good agreement between the model and experimental data. A set of Cartesian coordinates relating to the final refined structure is given in Table S6. The least-squares correlation matrix showing refined parameters with a correlation greater than or equal to 50% is provided as Supporting Information (Table S7).

Results and Discussion

The presence of two different heteroatoms in **2** and **3** is the principal reason for the change to C_s symmetry from the C_{2v} symmetry exhibited by **1**. The so-called *arachno* count is reflected in the molecular shapes: **2** and **3** display open six-membered faces in boat conformations, which is in accordance with the qualitative connectivity considerations of Williams.[24] Further convincing support for structures **2** and **3** comes from GIAO-SCF calculations (and to a greater extent from GIAO-MP2 calculations) of ^{11}B chemical shifts. The agreement with experiment is excellent in the case of **3** using GIAO-MP2/II, for both r_{h1} and r_e internal coordinates. The discrepancies between experimental and calculated ^{11}B chemical shifts for B(2) and B(4) in **2** are similar to those observed for two *arachno* clusters derived from **1**, namely *arachno*-6,5,9-$NC_2B_7H_{12}$ and *arachno*-6,5,10-$C_2NB_7H_{12}$.[25] It has also been noted that the experimental ^{11}B chemical shifts are solvent dependent. For neutral $B_{10}H_{14}$, differences in the range 0.2−2 ppm are typical depending on the solvent.[26]

Table 2. Calculated and Experimental NMR Chemical Shifts for *arachno*-6,9-CSB_8H_{12}, **2**, and *arachno*-6,9-CNB_8H_{13}, **3**[a]

	B(1,3)	B(2)	B(4)	B(5,7)	B(8,10)
		arachno-6,9-CNB_8H_{13}, **2**			
GIAO-HF/II//MP2[b]	−38.0	14.0	2.7	−23.3	−12.1
GIAO-HF/II//MP2[c]	−37.6	14.3	3.0	−22.8	−11.7
GIAO-MP2/II//MP2[b]	−39.3	8.3	−2.6	−28.0	−15.3
GIAO-MP2/II//MP2[c]	−38.9	8.6	−2.2	−27.5	−14.9
experimental[d]	*−41.6*	5.4	1.5	*−28.3*	*−15.7*
		arachno-6,9-CSB_8H_{12}, **3**			
GIAO-HF/II//MP2[b]	−33.7	15.7	11.2	−19.1	−9.0
GIAO-HF/II//MP2[c]	−33.5	15.6	11.5	−18.5	−8.7
GIAO-HF/II//GED	−33.5	16.1	12.3	−18.0	−8.3
GIAO-MP2/II//MP2[b]	−34.4	10.9	6.2	−22.7	−11.9
GIAO-MP2/II//MP2[c]	−34.1	10.8	6.5	−22.0	−11.5
GIAO-MP2/II//GED	−34.0	11.4	7.4	−21.5	−11.2
experimental[d]	*−34.1*	10.7	6.1	*−21.6*	*−12.6*

[a] Relative to $BF_3{\cdot}OEt_2$; for calculations, B_2H_6 was used as a primary reference. [b] Using the RMP2/6-31G* optimized geometry. [c] Using the RMP2/6-311++G** optimized geometry. [d] Reference 9.

The geometries of **2** and **3** are shown in Figures 2 and 3, respectively. Calculated parameters and, in the case of **3**, GED parameters are compared in Table 3. Despite the fact that sulfur is a second-row element, the calculated S(9)−B(8) and S(9)−B(10) bond lengths in **3** (193.6 pm at MP2/6-31G*) are only 4.2 pm longer than r[B(9)−B(10)] in **1** (189.4 pm). Thus, the size of the 8−9−10 angle has not changed much with respect to **1**,[11b,25] (98.7° compared to 101.5°). In contrast, the incorporation of carbon and nitrogen gives substantial deviations of the 5−6−7 and 8−9−10 triangles in **2** and the 5−6−7 triangle in **3** from that in **1**, in effect compressing the carbon and nitrogen atoms toward the center of the cluster. This flattening of the B(8)−N(9)−B(10) triangle[27] (this BNB angle is 122.8°) is even more pronounced than that of the corresponding B−C−B triangles (with BCB angles of 111.4° and 112.9° in **2** and **3**, respectively) and is accompanied by shorter C/N−B bonds than in **1** (see Table 3).

Closer inspection of the bond lengths to the heteroatoms reveals a second interesting feature of these heteroboranes. In **1**, the longest bond is B(5)−B(6) (189.4 pm) and its three symmetrical equivalents. In contrast, the adjacent bond, B(2)−B(6) is one of the shortest (174.9 pm), so that the difference between these two bond lengths is 14.5 pm (all MP2/6-31G* values). Replacement of B(6) with carbon results in a substantial reduction of the difference between these bonds to 8.1 and 8.7 pm in **2** and **3**, respectively. This effect is more pronounced when the heteroatom is nitrogen or sulfur, for which the respective values of [B(8)−X(9) minus B(4)−X(9)] are −3.4 and 0.1 pm in **2** and **3**, respectively. Perhaps even more surprising, however, is the lengthening of the B(4)−B(8) and B(4)−B(10) bonds relative to those in $[B_{10}H_{14}]^{2-}$. Substitution increases these bond lengths by 11.5 pm in **2** and 14.6 pm in **3**. However, the analogous increases in the B(2)−B(5) and B(2)−B(7) bond lengths of 2.7 pm in **2** and 1.8 pm in **3** are comparatively small.

(24) Williams, R. E. *Adv. Inorg. Chem. Radiochem.* **1976**, *18*, 95.
(25) Jelínek, T.; Štíbr, B.; Kennedy, J. D.; Hnyk, D.; Bühl, M.; Hofmann, M. *J. Chem. Soc., Dalton Trans.* **2003**, 1326.
(26) Gaines, D. F.; Nelson, C. K.; Kunz, J. C.; Morris, J. H.; Reed, D. *Inorg. Chem.* **1984**, *23*, 3252.

Table 3. Selected Geometrical Parameters for $[B_{10}H_{14}]^{2-}$, **1**, *arachno*-6,9-CNB_8H_{13}, **2** and *arachno*-6,9-CSB_8H_{12}, **3**[a]

	1 MP2/6-31G*	**2** MP2/6-31G*	**3** MP2/6-31G*	MP2/6-311++G**	GED
B(1)−B(2)	177.2	174.3	174.4	175.5	175.7(2)
B(1)−B(3)	180.6	180.3	179.3	180.3	180.7(2)
B(1)−B(4)	177.2	175.6	175.7	176.7	177.0(2)
B(1)−B(5)	177.1	181.3	180.8	182.0	182.3(2)
B(1)−B(10)	177.1	179.2	177.5	178.5	178.8(2)
B(2)−B(5)	174.6	177.3	176.4	177.6	178.0(2)
B(2)−C(6)	174.9	165.6	165.0	166.0	165.9(4)
B(4)−X(9)	174.9	157.8	193.5	194.4	194.8(4)
B(4)−B(10)	174.6	186.1	189.2	190.2	190.7(3)
B(5)−C(6)	189.4	173.7	173.7	174.0	174.2(2)
B(5)−B(10)	186.6	183.7	183.9	184.9	185.4(3)
X(9)−B(10)	189.4	154.4	193.6	193.8	194.6(3)
B(5)−C(6)−B(7)	101.5	111.4	112.9	113.4	113.2(3)
B(8)−X(9)−B(10)	101.5	122.8	98.7	99.2	98.9(2)
C(6)−B(5)−B(10)	114.6	110.3	111.3	111.1	111.7(4)
X(9)−B(10)−B(5)	114.6	115.3	117.8	117.3	117.7(2)
X(6)−B(5)···B(7)−B(8)	131.1	132.8	129.9	129.6	130.7(6)
X(9)−B(10)···B(8)−B(7)	131.1	144.6	136.9	136.2	136.8(3)

[a] Distances are in pm and angles, and torsions are in degrees.

Table 4. Selected Wiberg Bond Indices Computed from the MP2/6-31G* Electron Density and Corresponding Bond Lengths for **1**, **2**, and **3**[a]

	$[B_{10}H_{14}]^{2-}$ X = B, Y = B		CNB_8H_{13} X = C, Y = N		CSB_8H_{12} X = C, Y = S	
	index	length	index	length	index	length
B(2)−B(5)	0.53	174.6	0.38	177.3	0.39	176.4
B(2)−X(6)	0.54	174.9	0.57	165.6	0.58	165.0
B(5)−X(6)	0.54	189.4	0.61	173.7	0.61	173.7
B(4)−B(10)	0.53	174.6	0.28	186.1	0.36	189.2
B(4)−Y(9)	0.54	174.9	0.56	157.8	0.65	193.5
B(10)−Y(9)	0.54	189.4	0.68	154.4	0.79	193.6

[a] Bond lengths are in pm.

Inspection of the Wiberg bond indices[16] computed by the NBO program[17] (part of the Gaussian software) provides some insight into these effects, selected results of which are displayed in Table 4. The first thing to be noted is that, despite B(5)−B(6) being much longer than the other bonds in the parent compound, **1**, the bond indices are remarkably similar. The origin of this difference is presumably the smaller number of neighboring atoms. As can be expected, substitution of BH_2^- units significantly disrupts the bond indices in the vicinity of the substitution. With the exception of those to sulfur, all increases in bond index are accompanied by a reduction in bond length. The decrease in the bond length differences [B(5)−X(6) minus B(2)−X(6)] and [B(8)−X(9) minus B(4)−X(9)] on substitution appear to be the result of an increase in the electron density shared in the B(5)−X(6) and B(10)−X(9) bonds rather than a decrease in B(2)−X(6) and B(4)−X(9) bond strengths. The accompanying decrease in B(2)−B(5) and B(4)−B(10) bond indices (and corresponding increases in bond lengths) suggests that these bonds are the primary source of electron density for the strengthening of the B(5)−X(6) and B(4)−X(9) bonds in the open face.

In summary, all of the deformations occurring within **2** and **3** with respect to **1** are well described by the RMP2-(fc)/6-31G* parameters, which may be deemed to be good representations of the molecular geometries of **2** and **3**, as revealed by good fits between the computed and experimental ^{11}B chemical shifts. The GED structure of **3** lies 4 kJ mol^{-1} above the computed RMP2(fc)/6-311++G** structure as calculated at the same level. These energetic and magnetic criteria thus support the high quality of the experimentally determined geometry of **3**.

Acknowledgment. The support of the Ministry of Education of the Czech Republic (project LC523) is greatly appreciated. S.A.H. thanks the School of Chemistry for jointly funding a studentship with the EPSRC, who also funded the electron diffraction research (Grant No. GR/R17768) and currently fund D.A.W. and H.E.R. (Grant No. EP/C513649).

Supporting Information Available: Listings of GED data analysis parameters, selected distances, amplitudes of vibration, and perpendicular aplitude correction coefficients derived from or used in the GED refinement, the least-squares correlation matrix for the GED refinement, atomic coordinates for each structure and GED molecular scattering intensity curves. This material is available free of charge via the Internet at http://pubs.acs.org.

IC061253H